

## Effect of the Optical Bias on the a-Si:H Optical Demultiplexer Device

Miguel Fernandes, Manuela Vieira, Manuel A. Vieira, Paula Louro

Electronics Telecommunications and Computer Department  
ISEL  
Lisbon, Portugal  
mfernandes@deetc.isel.ipl.pt

Miguel Fernandes, Manuela Vieira, Manuel A. Vieira, Paula Louro

CTS  
UNINOVA  
Caparica, Portugal

**Abstract**—This paper presents results on the use of multilayered a-SiC:H heterostructures as a device for wavelength-division demultiplexing of optical signals. The devices presented enable the simplification of the optical front end system by using their intrinsic color selectivity to avoid the need of external optical filters. The device is composed of two stacked p-i-n photodiodes, each optimized for the absorption of a part of the optical spectrum. Band gap engineering was used to adjust the photogeneration and recombination rates profiles of the intrinsic absorber regions of each photodiode to short and long wavelength absorption and carrier collection in the visible spectrum. The photocurrent signal using different input optical channels (wavelengths) was analyzed at reverse and forward bias and under steady state illumination. A demultiplexing algorithm based on the voltage controlled selectivity of the device is proposed and tested. The operation frequency of the device was analyzed under different optical bias conditions. An electrical model of the WDM device is presented and supported by the solution of the respective circuit equations. The main application of these devices is in the field of optical communications that use the wavelength division multiplexing technique to encode multiple signals into the same transmission medium. Other possible applications of the device in optical communication systems are also proposed.

**Keywords**-WDM; Optical sensor; a-Si:H

### I. INTRODUCTION

Wavelength division multiplexing (WDM) devices are used when different optical signals are combined on the same optical transmission medium, in order to enhance the transmission capacity and the application flexibility of optical communication and sensor systems. The use of WDM technologies not only provides high speed optical communication links, but also offers advantages such as higher data rates and self-routing. The commercially available WDM devices usually include prisms, interference filters or diffraction gratings in order to separate the different channels. Currently modern optical networks use Arrayed Waveguide Grating (AWG) as optical wavelength (de)multiplexers [1] that use multiple waveguides to carry the optical signals. In this paper we report the use of a monolithic WDM device based on an a-Si:H/a-SiC:H multilayered semiconductor heterostructure. The device makes use of the fact that the optical absorption of the different wavelengths can be tuned by means of electrical

bias changes or optical bias variations. This capability is obtained using adequate engineering design of the multiple layers thickness, absorption coefficient and dark conductivities [2, 3].

### II. EXPERIMENTAL DETAILS

The device described herein operates in the 400 to 700 nm range which makes it suitable for operation at visible wavelengths in optical communication applications. The device is a multilayered heterostructure based on a-Si:H and a-SiC:H. The device is quite simple, consisting in a stack of two p-i-n structures sandwiched between two transparent electrical contacts (Fig. 1). Both front and back structures behave as optical filters confining, respectively, the absorption of the short and the long wavelength optical carriers, while the intermediate wavelengths are absorbed across both [4, 5]. The device was operated within the visible range using as optical signals three modulated light beams (with variable modulation frequency and intensity) supplied by red, green and blue LED's with wavelengths of 470 nm, 524 nm and 626 nm, respectively. An electrical model of the WDM device is presented and supported by the solution of the respective circuit equations. Other possible applications of the device in optical communication systems are also proposed.

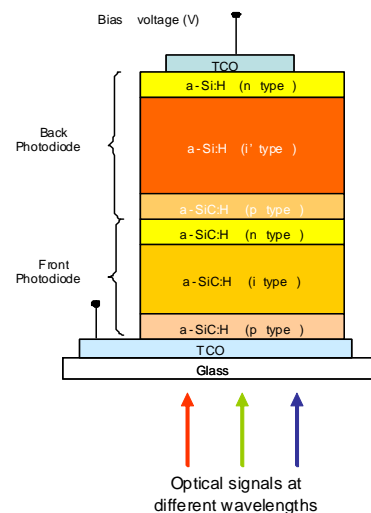


Figure 1. WDM device configuration.

The semiconductor layers were produced by Plasma Enhanced Chemical Deposition (PECVD) technique and optimized for specific wavelength sensitivity. The active device consists of a p-i'(a-SiC:H)-n/p-i(a-Si:H)-n heterostructure with low conductivity doped layers. The thicknesses and optical gap of the thin i'- (200nm; 2.1 eV) and thick i- (1000nm; 1.8 eV) layers are optimized for light absorption in the blue and red ranges, respectively. Transparent contacts have been deposited on front and back surfaces to allow the light to enter and leave from both sides (see Fig. 1).

To test the sensitivity of the device under different applied voltage and optical bias three modulated monochromatic lights beams: red (R: 626 nm; 51μW/cm<sup>2</sup>), green (G: 524 nm; 73μW/cm<sup>2</sup>) and blue (B: 470 nm; 115μW/cm<sup>2</sup>) and their polychromatic combinations (multiplexed signal) illuminated separately the device and the generated photocurrent was measured under positive and negative voltages (+1V<V<-10V), under or without steady state green optical bias (G: 524 nm; 73μW/cm<sup>2</sup>). The modulation frequency of each channel was chosen to be a multiple of the others in order to ensure a synchronous relation of ON-OFF states along each cycle and the optical powers were adjusted to give different signal magnitudes at -8V bias.

Fig. 2 displays the measured spectral photocurrent under reverse and forward bias. Results show that in the long wavelengths range (> 600 nm) the spectral response is independent on the applied bias while in the short wavelength the collection strongly increases with the reverse bias. As expected from Fig. 2, the red signal remains constant while the blue and the green ones decrease as the voltage changes from negative to positive. The output multiplexed electrical signal, obtained with the combination of the three optical sources, depends on both the applied voltage and on the ON-OFF state of each input optical channel. Under negative bias, there are eight separate levels while under positive bias they were reduced by half. The highest level appears when all the channels are ON and the lowest if they are OFF. Furthermore, the levels ascribed to the mixture of three or two input channels are higher than the ones due to the presence of only one (R, G, B).

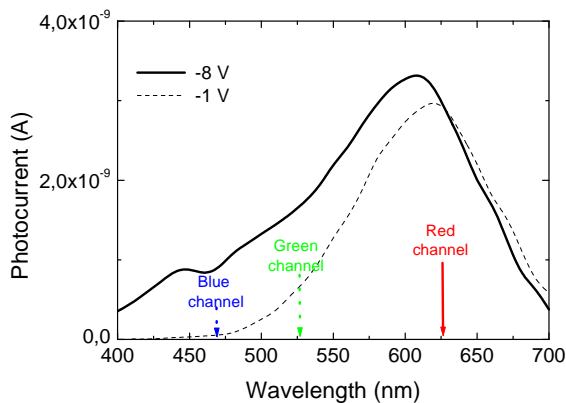


Figure 2. Spectral photocurrent under reverse and forward bias.

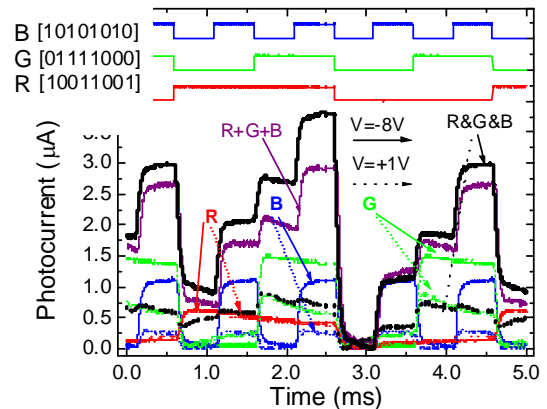


Figure 3. Single and multiplexed signals under negative (-8V) and positive (+1V) electrical bias.

An optical nonlinearity was detected; the sum of the input channels (R+B+G) is lower than the correspondent multiplexed signals (R&G&B). This optical amplification, mainly on the ON-ON states, suggests capacitive effects due to the time-varying nature of the incident lights. Under positive bias the levels are reduced by half since and the blue component of the combined spectra falls into the dark level, the red remains constant and the green one decreases.

To recover the transmitted information (8 bit per wavelength channel) the multiplexed signal, during a complete cycle, was divided into eight time slots, each corresponding to one bit where each independent optical signals can be ON (1) or OFF (0).

Under positive bias, the device has no sensitivity to the blue channel (Fig. 1-2), so the red and green transmitted information can be extracted. The highest level corresponds to both channels ON (R&G: R=1, G=1), and the lowest to the OFF-OFF stage (R=0; G=0). The two levels in-between are related with the presence of only one channel ON, the red (R=1, G=0) or the green (R=0, G=1). To distinguish between these two situations and to decode the blue channel, the correspondent sub-levels, under reverse bias, have to be analyzed. The highest increase at -8V corresponds to the blue channel ON (B=1), the lowest to the ON stage of the red channel (R=1) and the intermediate one to the ON stage of the green (G=1). Using this simple key algorithm the independent red, green and blue bit sequences can be decoded as: R[01111000], G[10011001] and B[10101010], as shown on the top of Fig. 2, which are in agreement with the signals used for the independent channels.

### III. INFLUENCE OF THE STEADY STATE OPTICAL BIAS

Fig. 4 shows the time dependent photocurrent signal measured under reverse (-8V, symbols) and forward (+1V, dotted lines) bias using different input optical signals without and with (λ<sub>L</sub>) red, green and blue steady state additional optical bias. Both optical signals and steady state bias were incident on the device by the side of the a-SiC:H

thin structure. The optical signals were obtained modulation of the LED driving current and the optical power intensity of the red, green and blue channels adjusted to 51, 90, 150  $\mu\text{W}/\text{cm}^2$ , respectively. The steady state light was generated by LED's driven at a constant current value (R: 290  $\mu\text{W}/\text{cm}^2$ , G: 150  $\mu\text{W}/\text{cm}^2$ , B: 390  $\mu\text{W}/\text{cm}^2$ ).

Results show that the blue steady state optical bias increases the signals carried out by the red (Fig. 4a) and the green channels (Fig. 4b) and reduces the signal of the blue channel (Fig. 4c). Red steady state optical bias has an opposite behavior, reinforcing the blue channel and decreasing the blue and the green channels. The green optical bias mainly affects the green channel, as the output signal is reduced while the signals of the red and blue channels show negligible changes.

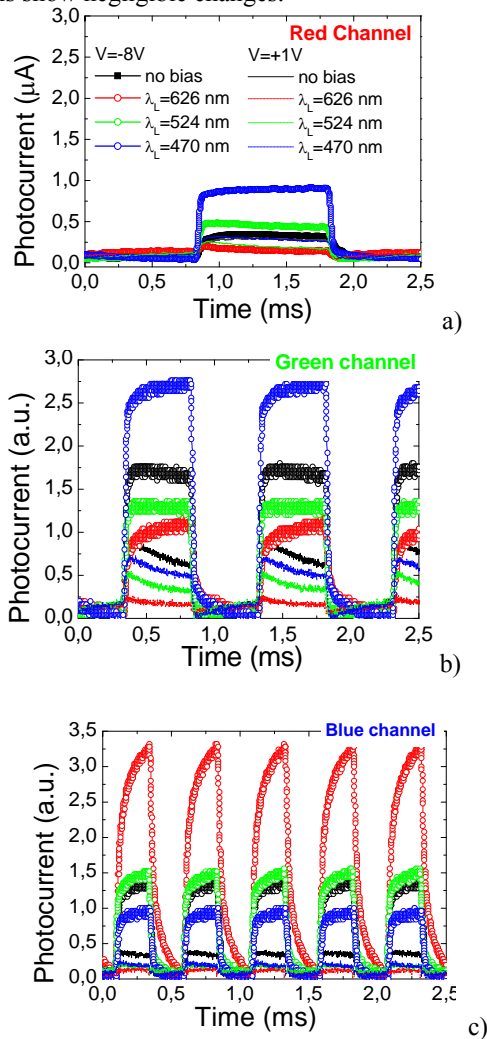


Figure 4. Red (a), green (b) and blue (b) channels under reverse and forward voltages without and with ( $\lambda_L$ ) red, green and blue steady state bias.

The behavior of the device under steady state optical bias can be explained attending to the dependence of the internal electric field distribution. When an optical bias is applied it mainly enhances the field distribution within the less photo excited sub-cell: the back under blue irradiation and the front under red steady bias. Therefore, the reinforcement of the electric field under blue irradiation and negative bias increases the collection.

The study of the modulation frequency influence on the device performance was analyzed through the spectral response of the device without and with steady state optical bias. Results are displayed in Fig. 5. Data from Fig. 5 show that without background light the curves measured under different modulation frequencies exhibit the same trend with two peaks located at 500 nm and 600 nm. The signal is reduced with the increase of the frequency. Under blue steady state illumination (Fig. 5b) the spectral response exhibits a different trend with a single peak located at 600 nm.

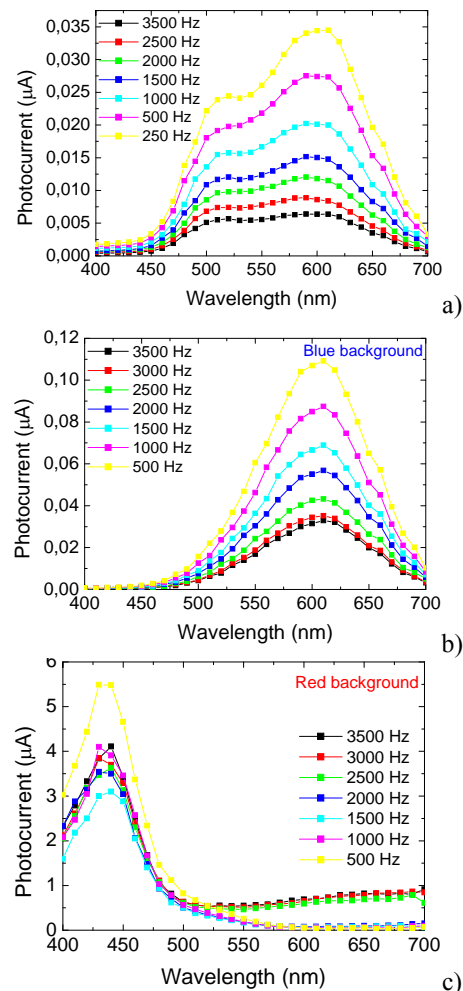


Figure 5. Photocurrent variation with the wavelength for different modulation frequencies at -8 V obtained: a) without, b) with blue, and d) with red background.

This is due to the strong attenuation of the short wavelengths (Fig. 4c). The red steady state illumination (Fig. 5c) has the opposite effect with a single peak at 500 nm. Under green background the spectral response shows two different regimes depending on the operation frequency. In the low frequency range the signal is similar to the trends obtained under red steady state light, while at higher frequencies it follows the behavior obtained without background light.

In Fig. 6 it is displayed the ratio of the signal measured under steady light and without it at different frequencies. Results show that at all frequencies of the analyzed range, under blue steady state illumination, the long wavelengths are amplified while shorter wavelengths (< 530 nm) are reduced. A similar result is observed for the red steady state illumination. Here the reinforcement of the signal level occurs for shorter wavelengths, while in the longer ones it is reduced.

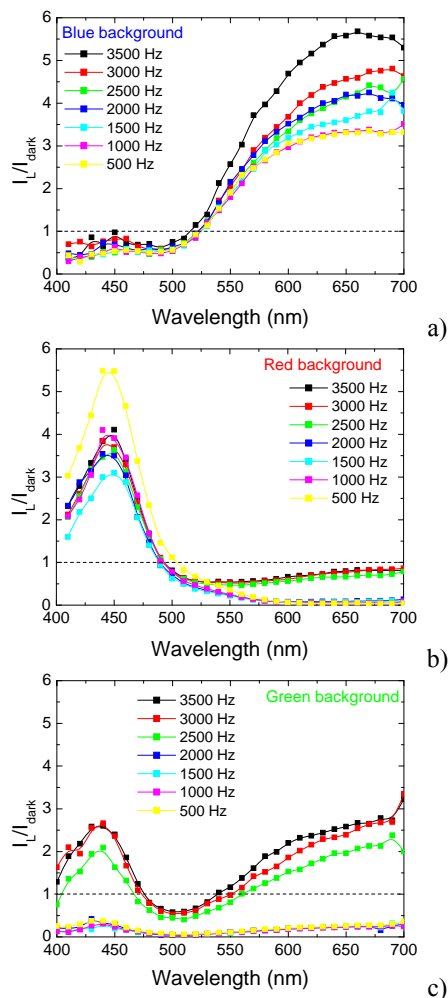


Figure 6. Ratio between the photocurrents under a) blue, b) red and c) green steady state illumination and without it (dark) at -8 V under different frequencies.

For the green background light the ratio between the photocurrents shows two different trends. At low frequencies the presence of the steady state light reduces the photocurrent, while for higher frequencies this reduction is only observed in a narrow range of the spectrum (from 470 nm up to 480 nm). In the remaining ranges the signal is enhanced. The maximum value observed for the amplification factor is around 3.

#### IV. OPTICAL BIAS CONTROLLED WAVELENGTH DISCRIMINATION

In Fig. 7, the input and the multiplexed channels, without or with green optical bias, are displayed at -8V. The bit sequence is shown at the top of the figure to guide the eyes. Results show that the presence of the optical bias reduces significantly the amplitude of green channel while a slightly increase is observed for the others two. The sum of the input channels (R+G+B) shows that when the green channel is ON no amplification occurs. This suggests that the green channel can be tuned by making the difference between the multiplexed signal without and with green irradiation (symbols).

This nonlinearity is due to the asymmetrical light penetration of the input channels and on the optical selectivity properties of the device. When an external optical bias is applied, it mainly influences the field distribution within the less photo excited sub-cell.

Under green light irradiation the electric field decreases on both sub-cells. So, some of the carriers generated by the green channel, also in both sub-cells, recombine and the collection decreases. When the red or blue channels are ON, the generation occurs only in one sub-cell. The electrical field, in the presence of the red and blue channels, lowers, respectively, in the back and front photodiodes (most absorbing cells), while the correspondent front and back photodiodes (less absorbing cells) reacts by assuming a reverse bias configuration compensating the effect of the green optical bias [7]. This self bias effect explains the slightly increase on the red and blue collection under green optical bias.

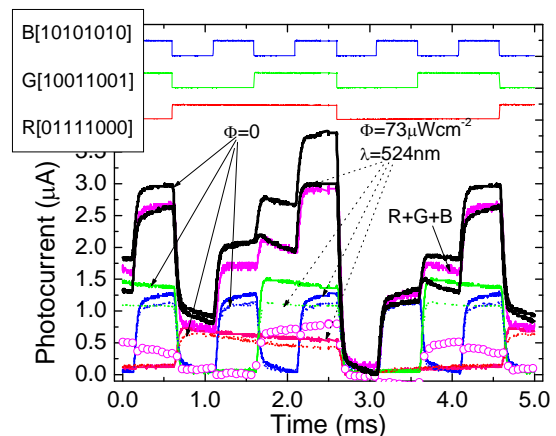


Figure 7. Single and combined signals @-8V; without (solid arrows) and with (dotted arrows) green optical bias.

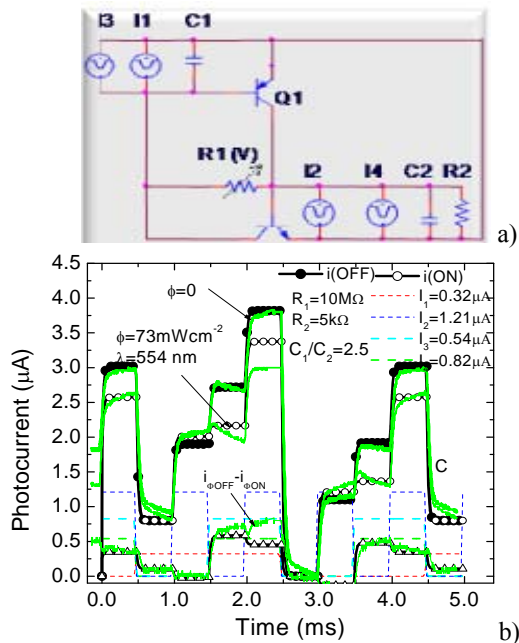


Figure 8. a) Electrical model, b) Simulated (symbols), current sources (dash lines) and experimental (solid lines) under +1V dc bias.

V. ELECTRICAL SIMULATION

The silicon-carbon pi<sup>+</sup>n/pin device can be considered as a monolithic double pin photodiode structure with two red and blue optical connections for light triggering. Based on the experimental results and device configuration an electrical model was developed [6]. Operation is explained in terms of the compound connected phototransistor equivalent model displayed as an inset in Fig. 8.

In Fig. 8 the currents under negative bias, with and without optical green bias, are compared. To simulate the green background, current sources intensities were multiplied by the on/off ratio between the input channels with and without optical bias (Fig. 6). The same bit sequence of Fig. 3 was used in both figures. To validate the model the experimental multiplexed signals are also shown (solid lines). Good agreement between experimental and simulated data was observed. The eight expected levels, under reversed bias, and their reduction under green irradiation are clearly seen.

When the pi<sup>+</sup>n/pin device is reverse-biased, the base emitter junctions of both transistors are inversely polarized and conceived as phototransistors, taking, so, advantage of the amplifier action of neighboring collector junctions which are polarized directly. This results in a charging current gain proportional to the ratio between both collector currents (C<sub>1</sub>/C<sub>2</sub>). Under positive bias the internal junction becomes always reverse-biased. If not triggered ON it is nonconducting, when turned ON by light it conducts like a photodiode, for one polarity of current.

Green irradiation moves asymmetrically voltages at the Q<sub>1</sub> and Q<sub>2</sub> bases toward their emitter values, resulting in lower values of I<sub>3</sub> and I<sub>4</sub> when compared without optical bias (Fig. 7). I<sub>1</sub> and I<sub>2</sub> slightly increase due to the increased carrier

generation on the less absorbing phototransistors. Under negative bias and during the duration of the red and blue pulses (I<sub>1</sub> or I<sub>2</sub> ON), as without optical bias, the internal junction remains forward biased and the transferred charge between C<sub>1</sub> and C<sub>2</sub> reaches the output terminal as a capacitive charging current. During the green pulse (I<sub>3</sub> and I<sub>4</sub> ON) only residual charges are transferred between C<sub>1</sub> and C<sub>2</sub>. So, only the charges generated in the base of Q<sub>2</sub> (I<sub>4</sub>) reaches the output terminal as can be confirmed by the good fitting between simulate and experimental differences of both multiplexed signals without and with optical bias.

VI. CONCLUSIONS

A double pi<sup>+</sup>n/pin a-SiC:H heterostructure with two optical sensitive regions sensitive to different spectral regions was presented. Multiple monochromatic communication channels, in the visible range, were transmitted together, each one with a specific bit sequence, and detected by the device. The combined optical signal was analyzed by reading out, under positive and negative voltages and optical green bias, the generated photocurrent across the device. Results show that the output multiplexed signal has a strong nonlinear dependence on the light absorption profile, i.e. on the incident light wavelength, bit rate, intensity and optical bias due to the self biasing of the junctions under unbalanced light generation profiles. By switching between positive and negative voltages the input channels can be recovered or removed.

The influence of the operation frequency was analyzed under different optical bias conditions. Further works on this topic is necessary for better understanding and further optimize the device operation.

ACKNOWLEDGMENT

This work was supported by FCT (CTS multi annual funding) through the PIDDAC Program funds and PTDC/EEA-ELC/115577/2009

REFERENCES

- [1] M. Bas, Fiber Optics Handbook, Fiber, Dev. and Syst. for Opt. Comm., Chap, 13, Mc Graw-Hill, 2002.
- [2] P. Louro, M. Vieira, Yu. Vygranenko, A. Fantoni, M. Fernandes, G. Lavareda, and N. Carvalho Mat. Res. Soc. Symp. Proc., 989 (2007) A12.04.
- [3] M. Vieira, M. Fernandes, P. Louro, A. Fantoni, Y. Vygranenko, G. Lavareda, and C. Nunes de Carvalho, Mat. Res. Soc. Symp. Proc., Vol. 862 (2005) A13.4.
- [4] P. Louro, M. Vieira, M.A. Vieira, M. Fernandes, A. Fantoni, C. Francisco, and M. Barata, Physica E: Low-dimensional Systems and Nanostructures, 41 (2009) 1082-1085.
- [5] P. Louro, M. Vieira, M. Fernandes, J. Costa, M. A. Vieira, J. Caeiro, N. Neves, and M. Barata, Phys. Status Solidi C 7, No. 3-4, 1188-1191 (2010).
- [6] M. A. Vieira, M. Vieira, M. Fernandes, A. Fantoni, P. Louro, and M. Barata, Amorphous and Polycrystalline Thin-Film Silicon Science and Technology 2009, MRS Proceedings Vol. 1153, A08-0.
- [7] M. Vieira, A. Fantoni, P. Louro, M. Fernandes, R. Schwarz, G. Lavareda, and C. N. Carvalho, Vacuum, Vol. 82, Issue 12, 8 August (2008), pp: 1512-1516.